Colloid Polym Sci (2004) 282: 1341–1346
DOI 10.1007/s00396-004-1051-1

ORIGINAL CONTRIBUTION

Tsuneo Okubo
Takehiro Miyamoto
Atsushi Otake
Mitsuhiro Suda
Akira Tsuchida

Seed polymerization of tetraethyl *ortho*-silicate in the presence of rod-like colloidal particles of anionic palygorskite and cationic β-FeO(OH)

Received: 21 August 2003
Accepted: 24 December 2003

T. Okubo (✉) · T. Miyamoto
A. Otake · M. Suda · A. Tsuchida
Department of Applied Chemistry and
Graduate School of Materials Science,
Gifu University, Yanagido 1-1,
Gifu 501-1193, Japan
E-mail: okubotsu@apchem.gifu-u.ac.jp
Fax: +81-58-293-2628

Abstract Kinetic analyses were made of the seed polymerization of tetraethyl *ortho*-silicate (TEOS) in the presence of rod-like colloidal particles of palygorskite and cationic β-FeO(OH) by turbidity and dynamic light-scattering measurements. Transmission electron microscopic measurements supported the formation of core-shell particles. The seed polymerization of TEOS took place exclusively on the surfaces of palygorskite. The main cause of the observation is due to the fact that the main component of palygorskite is SiO_2 and the affinity between palygorskite and TEOS is high, though the electrostatic repulsion between them is not favorable for shell formation. The shell formation of silica on a β-FeO(OH) particle also proceeded. The electrostatic attraction forces between the anionic polar TEOS monomers and cationic β-FeO(OH) particles played an important role in shell formation. These results are consistent with a polymerization mechanism consisting of the formation of small preliminary particles followed by their coalescence on the surfaces of the seeds to give the final large particles coated with silica layers.

Keywords Seed polymerization · Palygorskite · Iron(III) oxide hydroxide · Tetraethyl orthosilicate · Turbidity · Dynamic light scattering

Introduction

Monodispersed colloidal particles have provided most of the exciting and essential samples for studies in the field of colloidal science. The main purpose of this series of work is to synthesize hydrophilic and stable colloidal particles of any size and shape. As is well known, colloidal silica spheres are highly hydrophilic and disperse nicely without coagulation in water, especially in the deionized state with the coexistence of mixed beds of cation- and anion-exchange resins. However, syntheses of monodispersed and isotropic-shaped particles of silica are extremely difficult.

Aqueous suspensions of monodispersed polystyrene spheres having various sizes have been synthesized successfully and used in fundamental scientific research and also in industry. These spheres, however, are highly hydrophobic in water and apt to coagulate, especially when they contact hydrophobic substances such as air and plates made from poly(methyl methacrylate). On the other hand, colloidal particles of sparingly water-soluble electrolytic metal complexes such as tungstic acid (plate-like) and nickel dimethylglyoxime particles (rod-like) are highly monodispersed and anisotropic shaped. However, they dissociate into ionic species though their amount is very tiny, and are exchanged with H^+ and OH^- ions by the coexisting ion-exchange resins, resulting in the disappearance of the particles within several weeks! Furthermore, many biological substances are known to be monodispersed in their size and shape. A typical example of them is tobacco mosaic virus. However, the shape is not so stable in aqueous media, with the denaturation processes accompanied by conformational change. Taking account of these situations, polymerization reactions of monodispersed and stable colloidal spheres were obtained in our laboratory by coating seed particles of silica [1] and polystyrene spheres [2] with silica layers. In this report, seed polymerization of tetraethyl *ortho*-silicate (TEOS) on the surfaces of rod-like particles of palygorskite and β-FeO(OH) is described in detail.

There have been significant developments in techniques for colloidal silica synthesis and these have been accompanied by recent advances in the sol–gel method in the field of fine ceramics [3, 4, 5]. The synthesis of colloidal silica was first reported by Stöber et al. [6] in 1968, and was studied further by several researchers [7, 8, 9, 10, 11, 12, 13, 14, 15, 16, 17, 18, 19, 20]. The polymerization reaction is composed of the hydrolysis of silicate, Eq. 1, and then dehydration accompanied by three-dimensional cross-linking, Eq. 2.

$$\mathrm{Si(OC_2H_5)_4 + 4H_2O \rightarrow (OH)_4 + 4C_2H_5OH} \qquad (1)$$

$$\equiv \mathrm{SiOH + HO - Si} \equiv \rightarrow \equiv \mathrm{Si - O - Si} \equiv + \mathrm{H_2O} \qquad (2)$$

According to Shimohira and coworkers [9, 21] the primary small particles are formed first during an induction period, at the beginning of the reaction. Their critical size was estimated to be 10 to 20 nm [9]. The growing process with coalescence of the primary particles then follows, and the final silica spheres are formed.

Shimohira et al. proposed that the sixth-order of sphere size increases linearly with reaction time. It is recalled that the Lifshitz–Slyozov–Wagner theory supports the second- and third-order relations for the surface reaction-controlled and diffusion-controlled mechanisms, respectively [22]. Furthermore, fourth- and fifth-order relations have been proposed for the surface diffusion and the diffusion accompanied by dislocation in the cases of ceramics and metal formations, respectively [22, 23]. Several experiments, however, supported the sixth- or seventh-order relations [24, 25, 26], and theoretical explanation of the relationship was not so successful. Recently, a small-angle X-ray scattering study [20] revealed that after an induction period, the first particles to appear in the solution have a radius of gyration of ca. 10 nm and are mass fractals characterized by their polymeric open structure. The report did not support the growth model proposed so far by Shimohira and coworkers, for example. Ogihara [27] reviewed recent advances in the syntheses of colloidal silica spheres. We should note here that the kinetic mechanism of the formation reaction of the colloidal silica spheres from TEOS was studied in normal gravity [28] and also in microgravity [29].

Experimental

Materials

Palygorskite was a present from Professor Dr. Maria Stoimenova, Institute of Physical Chemistry, Bulgarian Academy of Science, Sofia, Bulgaria. The length and the thickness were 222 and 19 nm, respectively. The ζ-potential was −34.2 mV in water. The colloidal sample was deionized by coexistence with a mixed bed of cation- and anion-exchange resins [Bio-Rad, AG501-X8(D), 20–50 mesh] for more than 3 years before use.

Iron(III) oxide hydroxide, β-FeO(OH), particles (70 nm in length, 10 nm in thickness) were prepared by the very slow oxidation of a diluted aqueous solution of ferrous chloride kept at room temperature for 11 years [30]. The ζ-potential was +48.4 mV in water. The bottom layer of the stock suspension showed iridescent colors by Bragg diffraction from the array of rod-like particles.

Tetraethyl *ortho*-silicate (TEOS) was guaranteed grade and purchased from Wako Pure Chemicals (Osaka). Ethanol (C_2H_5OH, 99.5%) and ammonia (NH_3, 25%) were the most purified grade reagents commercially available and were obtained from Wako Chemicals. The water used for sample preparation was purified by a Milli-Q reagent-grade system (Milli-RO5 plus and Milli-Q plus, Millipore, Bedford, MA).

Electrophoretic light-scattering measurements

The ζ-potentials of the particles were measured on an electrophoretic spectrophotometer (ELS 8000, Otsuka Electronics, Osaka) at 25 ± 0.02 °C.

Turbidity measurements

Turbidity, i.e., absorbance, was taken on a spectrophotometer (Beckmann, DU650). Quartz optical cells (10×10×70 mm high) with long necks and screw caps were used for the kinetic turbidity measurements. The reaction was started by adding 1 mL TEOS in ethanol to the mixtures of ammonia and the seed particles in ethanol. Then the increase in the absorbance at 600 nm was measured.

Transmission electron microscopic measurements

The suspension (0.1 mL) was dried on a collodion mesh at room temperature before the transmission electron microscope (TEM, Hitachi, H8100) measurements.

Methods

Polymerization rates were obtained from the turbidity measurements. The total absorbance value, A, consists of the solvent absorption (A_0), the absorption from the particle formed (A_p), and the light scattering at θ (scattering angle) = 0 (A_s), i.e., Eq. 3 [1, 2].

$$A = A_0 + A_p - A_s \qquad (3)$$

The A_p term arising from the colloidal particles formed in the seed polymerization should increase linearly with increasing volume of the particle as:

$$A_p \propto Nld^2 \tag{4}$$

where N is the number of spheres formed in the reaction, and l and d are the length and the diameter of the rod particles, respectively. Equation 5 is derived using Eq. 4:

$$A_p = A_{\mathrm{shell}} + A_{\mathrm{seed}} \propto ld^2 \tag{5}$$

Here, A_{shell} and A_{seed} denote the absorbance contributed by the coated layers of silica and that from the seeds themselves.

It should be noted here that Eq. 3 holds only when the absorption dominates the scattering. When the latter is the case, $A_p \propto Nl^2d^4$ holds. The light-scattering term, A_s, is further approximated by Eq. 6,

$$A_s \propto \ln\left(I_p \times I_i + I_m\right) \tag{6}$$

where I_p is the intensity of the scattered light from the particle form factor at $\theta = 0$ and I_i is the intensity of scattered light contributed by the interference factor at $\theta = 0$. This term reflects the particle distribution in the reaction mixtures. I_m is the multiple-scattering term and is important especially in the final stage of the polymerization reaction, where large particles grow. The l (or d) value and the reaction rate, v, given by the growth rate of the particle size are, therefore, approximated very roughly by Eqs. 7 and 8, respectively, especially at the beginning of the polymerization reaction. However, it is highly plausible that the densities of the seed and the shell layer differ and the absorption should change with time. Thus, we should note that the analyses using Eqs. 7 and 8 are not so reliable and contain rather large errors.

$$l(\text{or } d) \propto A_p^{1/3} \tag{7}$$

$$v = \mathrm{d}l/\mathrm{d}t \propto \mathrm{d}A_p^{1/3}/\mathrm{d}t \tag{8}$$

Results and discussion

Seed polymerization of TEOS in the presence of anionic palygorskite particles

Figure 1 shows typical examples of the turbidity measurements for the seed polymerization reaction of TEOS in the presence of palygorskite (PGK) particles. The concentration of the seed particles ranges from zero to 0.001 vol%. Clearly, the reaction suspension became more turbid and the polymerization rate of TEOS increased as PGK concentration increased.

Figure 2 shows the term $A_p{}^{1/3} - A_{\mathrm{seed}}{}^{1/3}$ as a function of time. Clearly, the induction time, t_i, was zero in the presence of a large amount of palygorskite irrespective of the seed concentration, though t_i was observed in the absence of the seed particles. This observation supports strongly the view that the polymerization of TEOS proceeded exclusively on the surfaces of the seed spheres.

The polymerization rates of TEOS from the turbidity measurements shown in Fig. 3 were estimated using

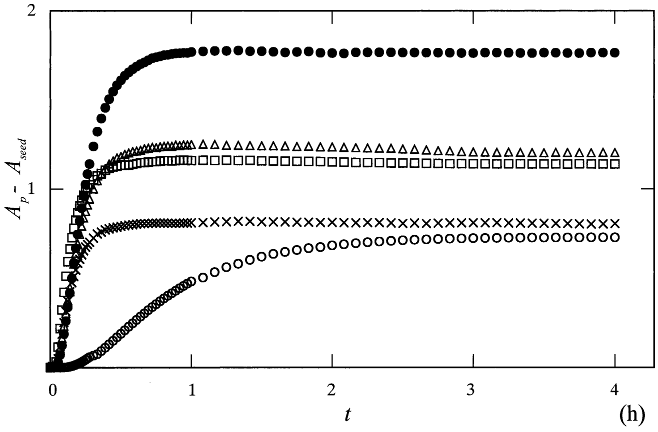

Fig. 1 Turbidity measurements in the course of seed polymerization of TEOS in the presence of palygorskite at 25 °C. [TEOS] = 0.5 vol%, [NH_3] = 3.0 wt%, at 600 nm; ○: [PGK] = 0 vol%, x: 1x10^{-6}, △: 1x10^{-5}, □: 1x10^{-4}, ●: 1x10^{-3}

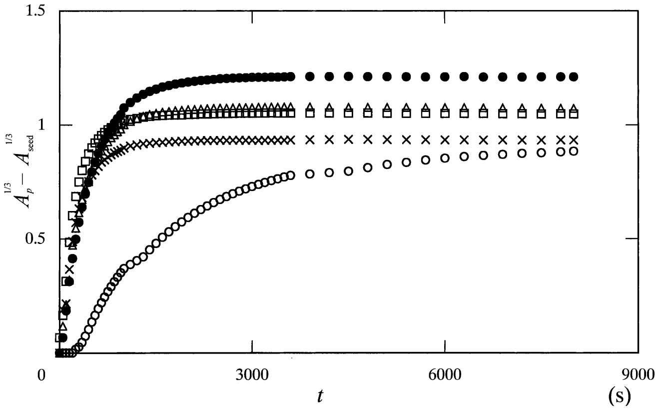

Fig. 2 Cube-root plots of the absorbance against time for the seed polymerization at 25 °C. [TEOS] = 0.5 vol%, [NH_3] = 3.0 wt%, at 600 nm; ○: [PGK] = 0 vol%, x: 1x10^{-6}, △: 1x10^{-5}, □: 1x10^{-4}, ●: 1x10^{-3}

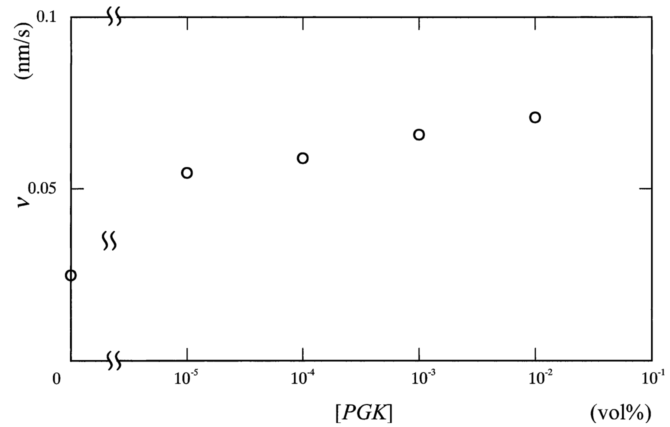

Fig. 3 Polymerization rates of TEOS in the presence of palygorskite at 25 °C. [TEOS] = 0.5 vol%, [NH_3] = 3.0 wt%, at 600 nm

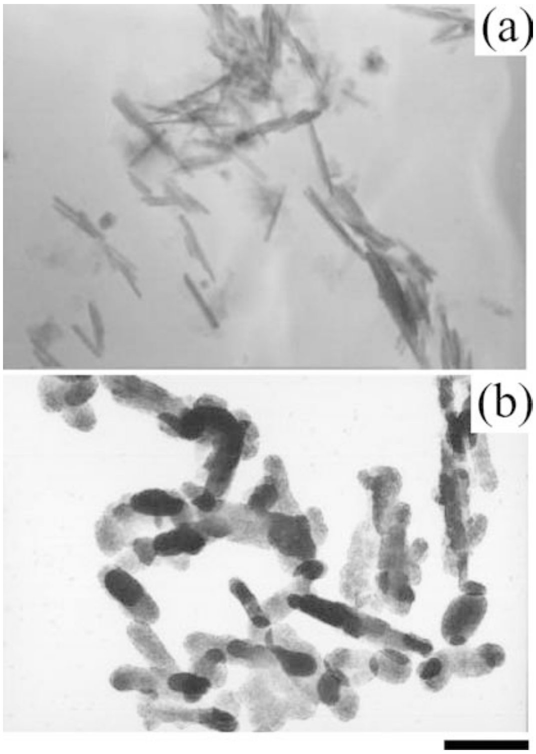

Fig. 4a,b TEM pictures of the particles formed in the presence of palygorskite; [PGK] = 0.001 vol%. **a** Before polymerization (PGK only). **b** After polymerization. Length of the *bar* is 300 nm

Eq. 8, from the reciprocal period between the intersections of the linear line with the initial and final horizontal lines in the cube root of the absorbance term A_p versus time plots. The growth rates of the shell layers increased as the concentration of the seed particles increased. These results are consistent with the reaction mechanism that the very small preliminary particles are formed first and then coalesce. It should be mentioned here that the affinity between the seeds and the preliminary particles is strong, and the coalescence and shell formation occur exclusively on the surface of palygorskite.

The shell formation of silica on the seed spheres was observed directly by the TEM pictures of the suspensions after the polymerization was completed. Figure 4 shows the TEM pictures of the particles before polymerization (Fig. 4a) and after polymerization in the presence of palygorskite (Fig. 4b). Clearly, the width after polymerization was about twice that before polymerization, and all the seed rods were coated with the silica shell homogeneously. This result also supports strongly the view that shell formation proceeded exclusively on the seed particles. It should be recalled here that the seed polymerization of TEOS also proceeded exclusively on the surface of a silica sphere [1]. The main component (ca. 50%) of palygorskite is SiO_2, so the high affinity between palygorskite and TEOS is highly plausible.

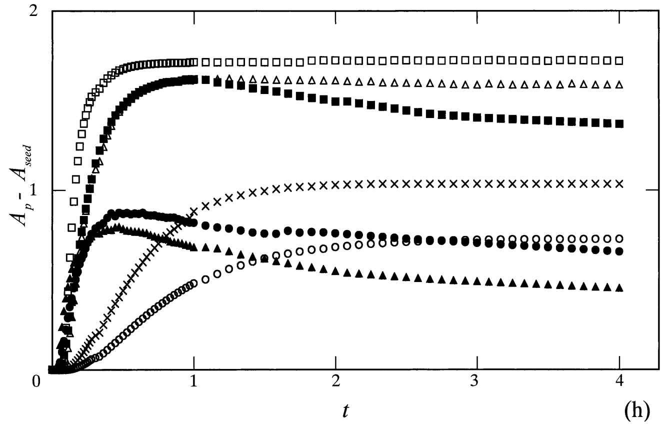

Fig. 5 Turbidity measurements in the course of seed polymerization of TEOS in the presence of *β*-FeO(OH) at 25 °C. [TEOS] = 0.5 vol%, $[NH_3]$ = 3.0 wt%, at 600 nm; ○: [*β*-FeO(OH)] = 0 wt%, x: 0.001, △: 0.005, □: 0.0075, ●: 0.01, ▲: 0.03, ■: 0.05

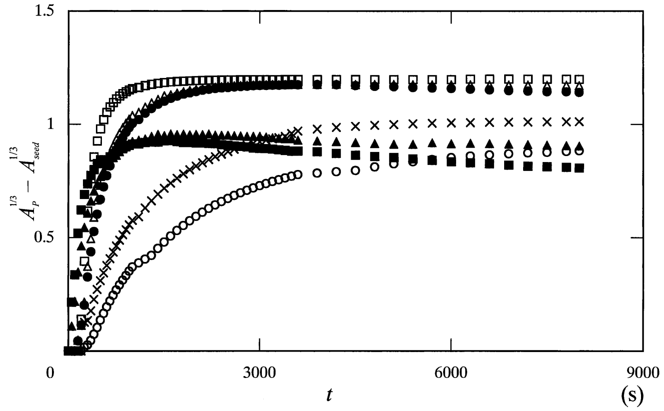

Fig. 6 Cube-root plots of the absorbance against time for the seed polymerization at 25 °C. [TEOS] = 0.5 vol%, $[NH_3]$ = 3.0 wt%, at 600 nm; ○: [*β*-FeO(OH)] = 0 wt%, x: 0.001, △: 0.005, □: 0.0075, ●: 0.01, ▲: 0.03, ■: 0.05

Seed polymerization of TEOS in the presence of cationic *β*-FeO(OH)

Figure 5 shows typical examples of the turbidity measurements for the seed polymerization reaction of TEOS in the presence of *β*-FeO(OH) particles. The concentration of the seed particles ranges from zero to 0.05 wt%. A_p–A_{seed} decreased after passing a maximum in the presence of a large amount of *β*-FeO(OH). This shows that the product particles from the seed polymerization sediment in part in the observation cell.

Figure 6 shows that the term $A_p^{1/3}$–$A_{seed}^{1/3}$ increased linearly with time. The induction time, t_i, shown in Fig. 7a decreased quickly as the seed concentration increased, though the induction time was large in the

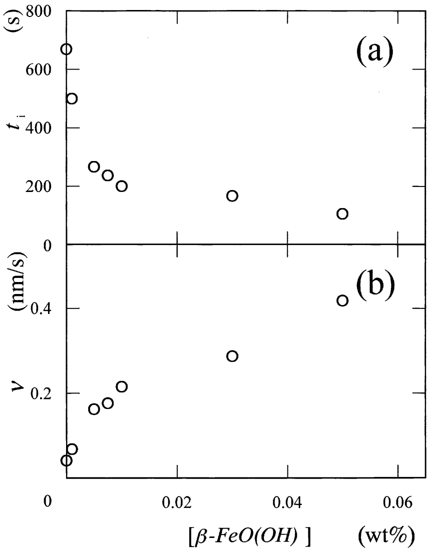

Fig. 7a,b Induction periods (**a**) and polymerization rates (**b**) for the seed polymerization of TEOS in the presence of β-FeO(OH) at 25 °C. [TEOS] = 0.5vol%, [NH_3] = 3.0 wt%, at 600 nm

absence of the seed particles. This observation supports strongly the view that the polymerization of TEOS proceeded exclusively on the surfaces of the seed β-FeO(OH) particles. It is highly plausible that the electrostatic attraction between the cationic seed particles and the anionic polar TEOS played an important role in the high polymerization rates.

The polymerization rates of TEOS on the surfaces of β-FeO(OH) particles from the turbidity measurements are shown in Fig. 7b using Eq. 8, from the reciprocal period between the intersections of the linear line with the initial and final horizontal lines in the cube root of the absorbance term A_p versus time plots. The growth rates of the shell layers increased significantly as the concentration of the seed particles increased. These results are consistent with the reaction mechanism that the very small preliminary particles are formed first and then coalesce. It should be mentioned here that the affinity between the seeds and the preliminary particles is strong, and the coalescence and shell formation occur mainly on the surface of β-FeO(OH) particles.

The shell formation of silica on the β-FeO(OH) particles was observed directly by the TEM pictures of the suspensions after the polymerization was completed. Figure 8 shows the TEM pictures of the particles before polymerization (Fig. 8a) and after polymerization in the presence of β-FeO(OH) (Fig. 8b). Clearly, most of the seed particles were coated with the silica shell, though the core-shell particles are associated to each other in this picture. This result also supports strongly the view that shell formation proceeds on the cationic seed particles by the electrostatic attraction forces between anionic polar TEOS monomers and cationic β-FeO(OH) particles. It should be noted here that a silica sphere was observed among the rod-shaped particles in the picture of Fig. 8b. This supports the hypothesis that the polymerization of TEOS proceeded independently apart from the seed particles, though the fraction of the spheres is very small. The coexistence of the spheres is due to the fact that the amount of TEOS was too large compared with that of β-FeO(OH) seeds under our experimental conditions.

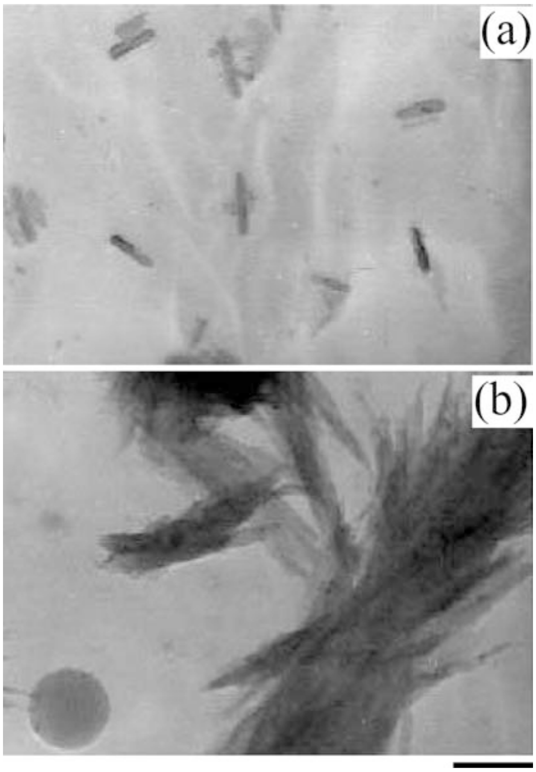

Fig. 8a,b TEM pictures of particles formed in the presence of β-FeO(OH); [β-FeO(OH)] = 0.005 wt%. **a** Before polymerization (β-FeO(OH) only). **b** After polymerization. Length of the *bar* is 100 nm

Acknowledgments The authors appreciate deeply Professor Dr. Maria Stoimenova for her kind provision of the palygorskite particles. The Ministry of Education, Science, Sports and Culture is thanked for Grants-in-Aid for Scientific Research on Priority Area (A) (11167241) and for Scientific Research (B) (11450367).

References

1. Okubo T, Miyamoto T, Umemura K, Kobayashi K (2001) Colloid Polym Sci 279:1236
2. Okubo T, Miyamoto T, Umemura K, Noguchi T, Kobayashi K, Tsuchida A (2003) Colloid Polym Sci 281:1055
3. Iler RK (1979) The chemistry of silica. Wiley, New York
4. Klein LC (ed) (1988) Sol–gel technology for thin films, fibers, preforms, electronics, and specialty shapes. Noyes, Park Ridge
5. Bergna HE (1994) The colloid chemistry of silica. Am Chem Soc, Washington
6. Stöber W, Fink A, Bohn E (1968) J Colloid Interface Sci 26:62
7. van Helden AK, Vrij A (1980) J Colloid Interface Sci 78:312
8. Kops-Werkhoven MM, Fijnant HM (1980) In: Degiorgio V, Corti M, Giglio M (eds) Light-scattering in liquids and macromolecular solutions. Plenum, New York, p 81
9. Shimohira T, Ishijima H (1981) Jpn J Chem Soc 9:1503
10. Okubo T (1988) J Chem Phys 88:6581
11. Matsoukas T, Gulari E (1988) J Colloid Interface Sci 124:252
12. Matsoukas T, Gulari E (1989) J Colloid Interface Sci 132:13
13. Bogush GH, Zukoski IV CF (1991) J Colloid Interface Sci 142:1
14. Bogush GH, Zukoski CF IV (1991) J Colloid Interface Sci 142:19
15. van Blaaderen A, van Geest J, Vrij A (1992) J Colloid Interface Sci 154:481
16. van Blaaderen A, Kentgens APM (1992) J Non-Cryst Solids 149:161
17. Okubo T (1992) Ber Bunsenges Phys Chem 96:61
18. Giesche H (1994) J Eur Ceram Soc 14:189
19. Lee K, Look JL, Harris MT, Mc Cormick AV (1997) J Colloid Interface Sci 194:78
20. Boukari H, Lin JS, Harris MT (1997) J Colloid Interface Sci 194:311
21. Shimohira T, Komuro N (1976) Powder Powder Metall 23:137
22. Shewnon PG (1964) Trans Met Soc AIME 230:1134
23. Nichols FA (1966) J Appl Phys 37:4599
24. Heg AW, Livey DT (1966) Trans Brit Ceram Soc 65:626
25. Kotera Y, Saito T, Terada M (1963) Bull Chem Soc Jpn 36:2195
26. Aihara K, Chaklader ACD (1975) Acta Metall 23:855
27. Ogihara T (2000) In: Sugimoto T (ed) Fine particles. Synthesis, characterization, and mechanisms of growth. Marcel Dekker, New York, p 35
28. Okubo T, Kobayashi K, Kuno A, Tsuchida A (1999) Colloid Polym Sci 277:483
29. Okubo T, Tsuchida A, Kobayashi K, Kuno A, Morita T, Fujishima M, Kohno Y (1999) Colloid Polym Sci 277:474
30. Watson JHL, Cardel RR Jr, Heller W (1962) J Phys Chem 66:1757